An ultra-Structural and cytological study of preimplantation development of the mouse

ARTICLE *in* JOURNAL OF EXPERIMENTAL ZOOLOGY · JULY 1969

DOI: 10.1002/jez.1401710303 · Source: PubMed

An Ultrastructural and Cytological Study of Preimplantation Development of the Mouse [1]

PATRICIA G. CALARCO [2,3] AND EDWARD H. BROWN
Department of Zoology, University of Illinois, Urbana, Illinois 61801

ABSTRACT Each stage of preimplantation development in the mouse from the fertilized egg to the blastocyst stage (including the unfertilized egg) was studied cytologically and ultrastructurally. Observations were made on the appearance and elaboration of several cellular organelles, inclusions and cell surface specilizations. The fertilized egg exhibits many intranuclear annulate lamellae, an increase in cytoplasmic vesicle number when compared to the unfertilized egg, and small amounts of crystalloids; mitochondria are vacuolated and small. The 2-cell stage is very similar to the fertilized egg but shows an increase in the number of cytoplasmic vesicles. The 4-cell stage is characterized by many changes: functional nucleoli appear, vacuolated mitochondria enlarge, cytoplasmic vesicles continue to increase in number, rough endoplasmic reticulum appears (as mitochondria-associated sacs), and some ribosomes are localized near the plasma membrane. At the 8-cell stage, large numbers of free ribosomes are observed in the cytoplasm, but clusters (polysomes) predominate at the 16-cell stage (morula). Morulae develop junctional complexes and exhibit differences in cytoplasmic basophilia between cells, which may be a prelude to differentiation. At the blastocyst stage, nucleoli change to an elongate form and differences in cytoplasmic background density can be observed ultrastructurally. Observations suggest that the contents of the blastocoel may be derived from the cytoplasmic vesicles, which increase in number and size subsequent to fertilization and discharge their contents into the intercellular spaces; the blastocoel arises as these fluid-filled spaces become confluent and enlarge.

The preimplantation development of the mouse occurs within approximately 100 hours, during which time at least six stages of development can be recognized: fertilized egg, 2-cell stage, 4-cell stage, 8-cell stage, morula and blastocyst.

Ovarian oocytes reach metaphase of the second meiotic division just before ovulation, and remain in this stage until fertilization. Fertilization occurs in the upper end of the oviduct and the second polar body is formed two to three hours after fertilization. Cleavage is total, slightly unequal, nearly synchronous, and occurs within the oviduct. The first cleavage occurs approximately 24 hours after mating; the intervals between succeeding cell divisions are about 12 hours. Embryos of 16 cells or more with no cavity are termed morulae and during this stage the embryos usually pass into the uterus. At approximately the 32-cell stage, a fluid-filled cavity forms between the cells of the morula and enlarges to become the blastocoel. Embryos are now termed blastocysts and will implant in the uterus approximately four and one-half days after fertilization (Snell and Stevens, 1966).

Normal morulae undergo certain changes prior to blastocoel formation. Lewis and Wright ('35) reported that the "clear yolk globules" of the 8-cell embryo increase in size and decrease in number by the morula stage, and are considerably reduced in number in the blastocyst. Mintz ('64b) observed that the cytoplasm of morulae becomes more translucent, and discrete bodies or vacuoles varying in density and surrounded by a membrane or interface appear; this is followed by the appearance of small, randomly distributed cavities which become confluent and enlarge. Melissinos ('07) described globules (glänzenden Tropfen) located near the intercellular spaces of the young blastocyst and suggested that these globules contain the blastocoel fluid. Huber

[1] This work was supported by a National Institutes of Health Predoctoral Fellowship, 1-F1-GM-24,170-04 and a U.S.P.H.S. Postdoctoral training grant PH-1T1-GM-941, awarded to P. G. Calarco and (in part) by a grant to E. H. Brown from the Graduate College Research Board of the University of Illinois.

[2] This work is based on part of a dissertation submitted by the senior author to the Graduate College of the University of Illinois in partial fulfillment of the requirements for the Ph.D. degree.

[3] Present address: Department of Biological Structure, University of Washington, Seattle, Washington.

('15), however, was unable to detect such globules. Smith ('56) suggested that there are two distinct layers of cells within the morula: an inner mass of rounded cells, and a covering layer, one cell thick, of smaller flattened cells, with the blastocoel first appearing between these two layers. Details of the process of blastulation are unknown.

Mintz ('64c) has demonstrated, by fusing morulae *in vitro*, that cleavage in the mouse is indeterminate. The regulative capacity of the embryo has not been investigated subsequent to the morula stage, when, as will be shown in this paper, intercellular junctions are formed.

Mice have an extended dependent period *in utero* and the oocyte contains little in the way of recognized yolky substances. Therefore, an early requirement for ribosomes and protein synthesis might be expected. Changes in RNA content during early cleavage of the mouse were investigated by Flax ('53), using cytophotometric measurements of Azure B stained sections. He found that the RNA content per embryo does not increase until after the appearance of stainable nucleoli at the 5 to 6-cell stage. Mintz ('64a) and Monesi and Salfi ('67), measuring H^3-uridine incorporation, suggested that RNA synthesis occurs in all preimplantation stages, with a notable increase in RNA synthesis occurring in the late morula stage. Ellem and Gwatkin ('68) also reported an increase in precursor incorporation at the morula stage. Incorporation of H^3-uridine into nucleoli begins at the 4-cell stage (Mintz, 64a). Assuming that the cistrons for ribosomal RNA are located within the nucleolar organizer, this incorporation reflects the onset of ribosomal RNA synthesis and is the earliest known activation of the nucleolar organizer region. Other studies by Mintz ('64a) demonstrated that DNA synthesis (H^3-thymidine incorporation) and protein synthesis (H^3-leucine incorporation) also occur in all preimplantation stages.

A few cytological studies exist for the mouse (Sobotta, 1895; Lewis and Wright, '35) and the rat (Melissinos, '07; Huber, '15), a close relative of *Mus musculus*. However, these studies deal primarily with the timing of cleavage, and the size, shape and location of the embryo, and include only limited observations of cellular organelles and developmental changes during cleavage.

Few ultrastructural descriptions of murine preimplantation stages have been published. Yamada et al. ('57) studied the ovarian oocytes of the mouse. Electron micrographs of mouse blastocysts have been published in a comparative study of blastocysts (Enders and Schlafke, '65).

Several ultrastructural studies of rat preimplantation stages are available. Sotelo and Porter ('59) studied the fine structure of unfertilized and fertilized ova and 2-cell stages. Izquierdo and Vial ('62) extended their own study to the 8-cell stage. Electron micrographs of 2-cell, 8-cell and blastocyst stages of the rat have been published (Schlafke and Enders, '63; Enders and Schlafke, '65). Mazanec and Dvorak ('63) published a short ultrastructural paper covering rat development from the fertilized egg to the blastocyst, and Mazanec ('65) later published a detailed ultrastructural investigation of rat preimplantation development.

A cytological and ultrastructural examination of normal preimplantation stages of the mouse, using improved methods of fixation and epoxy resin embedding, was undertaken to provide a more detailed account of cellular structure and perhaps provide insight into cellular interactions during the early development of the mouse. This paper presents observations on the ovulated unfertilized egg and preimplantation stages, with attention focused on the types and structure of organelles present and the changes that take place from fertilization to blastulation.

MATERIALS AND METHODS

The ova and embryos used in this study were obtained from crosses of Bagg albino (BALB/c) males and females maintained at a temperature of approximately 23.5°C. The light-dark cycle was automatically controlled and was adjusted to provide 14 hours of light and 10 hours of darkness.

A modification of the technique of Edwards and Gates ('59), as described in another paper (Calarco and Brown, '68), was used to induce superovulation in ma-

ture females. The use of superovulation increased the number of embryos obtained and also permitted staging on the basis of age. Embryonic age (in hours) was figured from the time of ovulation, which was considered to have occurred 12 hours after the injection of chorionic gonadotropin.

Ovaries, oviducts and uterine horns were removed from pregnant females and placed in Brinster's culture medium without BSA (Brinster, '65a), hereafter designated BCM. Embryos were flushed from the uterus into a depression slide, washed twice with BCM, and examined at 500 × with phase contrast optics to determine the approximate number of cells present in each embryo. Subsequent fluid changes were carried out with the embryos in a modified version of the microchamber devised by Izquierdo ('67).

Embryonic cells are typically difficult to preserve adequately for electron microscopic examination. Therefore, at the onset of this investigation several fixation procedures were used which varied in the type and concentration of fixative, the composition of the buffer, and the time of fixation (Calarco, '68).

Pre-fixation incubation at room temperature for 6 minutes in BCM containing 0.5% Pronase (Calbiochem), heated to 37°C prior to use, was employed to partially remove the zona pellucida (Mintz, '62). This treatment seemed to permit more rapid penetration of the fixative and did not appear to alter the ultrastructure of the embryos (Calarco, '68). In addition, abnormal or degenerate eggs were susceptible to the enzymatic action of Pronase and were reduced to cellular debris, thus removing them from the sample to be studied.

Since the mouse embryo is reported to develop optimally *in vitro* at an osmolality of 276 milliosmols and a pH of 6.82 (Brinster, '65b), it was at first assumed that an ideal fixative should be similar in osmolality and pH. However, the fixation procedure which consistently provided the best preservation of ultrastructural details (Calarco, '68) used solutions having an osmolality of 550 milliosmols and a pH within 6.8–7.4 (prepared according to the data reported by Maser et al., '67). Thus, most of the observations presented in this paper were of ova and embryos treated with Pronase, fixed for 30 minutes in 3% glutaraldehyde in 0.1 M phosphate buffer, and postfixed for 15 minutes in 2% osmium tetroxide in 0.1 M phosphate buffer. Ova and embryos were then rapidly dehydrated through a cold ethanol series and embedded in EPON 812 by a modification of the procedure described by Luft ('61).

Procedures employed in the sectioning, mounting and staining with Azure B bromide (0.025% at pH 4) of serial sections 2 μ thick for light microscopy have been described previously (Calarco and Brown, '68).

Thin sections for electron microscopy were cut with a diamond knife on an LKB Ultratome. Contrast was enhanced by treating the sections with saturated uranyl acetate (Watson, '58) followed by lead citrate (Reynolds, '63). Grids were examined with a Hitachi HU11-A electron microscope.

Spherical cytoplasmic vesicles, approximately 1 μ in diameter, were counted at different stages of development in 2 μ serial sections of embryos stained with Azure B. Counting was carried out at a magnification of 1250 × using phase contrast optics and a red filter. One ocular was fitted with a grid micrometer to simplify the counting procedure and the other ocular contained a linear micrometer which was used to determine the diameters of cells and cytoplasmic vesicles.

OBSERVATIONS

Observations on normal development will be presented for the following stages: unfertilized eggs (six hours after ovulation, determined as explained in Materials and Methods), fertilized eggs—pronuclear stages and stages just prior to the first cleavage (24 hours), 2-cell embryos (24–26 hours), 4-cell embryos (49–60 hours), 8-cell embryos (53 hours), morulae (70 hours) and blastocysts (70 and 81 hours).

Light Microscopy

Three types of cytoplasmic entities are visible in embryos sectioned and stained for study with the light microscope: (1) clear cytoplasmic vesicles (V); (2) dark-staining crystalloids (C); and (3) medium-

density areas (J) (figs. 1–8). Cytoplasmic vesicles and crystalloids can be seen in living embryos observed with phase contrast optics, but their relative numbers and distribution are not readily apparent.

Cytoplasmic vesicles (V) are spheres of approximately 1 μ in diameter which contain a substance of medium density. Some of the contents of the vesicles appear to be lost during the fixation or dehydration procedures, which accounts for their clear appearance in sectioned material. The distribution of cytoplasmic vesicles appears to be random in the unfertilized ovum, the early pronuclear stage, and the 2-cell stage. Subsequent to the 4-cell stage, they tend to be localized near contiguous cell boundaries. In morulae, cytoplasmic vesicles are occasionally found in the peripheral cells of the embryo, but the internal cells exhibit a higher concentration of these vesicles (fig. 6). In the blastocyst very few cytoplasmic vesicles are detected. In morulae and blastocysts, internal cells are often separated by small spherical distentions of the intercellular spaces (figs. 6, 8).

The diameter of vesicles in embryos younger than the 4-cell stage is generally less than 1 μ, as determined by electron microscopy. Measurements made on electron micrographs suggest an average vesicle diameter of 0.7 μ, with a range from 0.4 μ to 0.9 μ, for unfertilized and fertilized eggs, and an average vesicle diameter of 0.9 μ, with a range from 0.7 μ to 1.1 μ, for the 2-cell stage. At the 4-cell stage, vesicle diameters are approximately 1 μ; older stages possess vesicles ranging in diameter from 1.5 μ to 3 μ, as determined by light microscopy.

An attempt was made to obtain quantitative estimates of changes in the number of these vesicles per cell in various preimplantation stages. Although such data were obtained, the variability introduced by different genotypes, and by the nonequivalence in age of similar stages from different BALB/c matings, made it difficult to obtain results amenable to statistical analysis (Calarco, '68). However, some general observations from these results are pertinent to the present paper. The number of cytoplasmic vesicles per cell increases progressively from the unfertilized egg to the 4-cell stage. After the 4-cell stage the number of vesicles decreases and continues to decrease in older embryos.

Crystalloids (which will be discussed later on the basis of ultrastructural observations) are not observed in the unfertilized or fertilized egg, the 2-cell stage or 4-cell stage. In the 8-cell stage some crystalloids are visible, and from the 8-cell stage to the morula, crystalloids increase in number and size (figs. 6, 7).

Medium-density areas (J), which stain more intensely than the surrounding cytoplasm, are observed frequently in the unfertilized egg (fig. 1). Although electron microscopic observations (to be described below) indicate that these areas are present in all preimplantation stages, they become difficult to identify with the light microscope as other cytoplasmic components accumulate.

Prior to the blastocyst stage there appears to be little difference in cytoplasmic basophilia (Azure B staining) between stages, but cytoplasmic basophilia is considerably more pronounced in cells of the blastocyst than in any earlier stage. In addition, trophoblast cells appear to stain more intensely with Azure B than do cells of the inner cell mass (fig. 8). The cells of individual morulae often exhibit differences in cytoplasmic basophilia (fig. 7). These differences are not observed in embryos younger than the morula stage.

Nucleoli are present from the pronuclear stage to the blastocyst and stain intensely with Azure B. However, the number, size and shape of nucleoli change as development progresses. There are several spherical "nucleoli" present in the pronuclei of the fertilized egg (fig. 2), and the nuclei of the 2-cell stage (fig. 3). At the 4-cell stage, nucleoli are fewer in number, with one to three nucleoli appearing larger than the rest. Nucleoli of 4-cell embryos are not as extremely rounded as those of the 2-cell stage, but are roughly spherical and have projections which occasionally reach the nuclear envelope. At this stage the nucleolus can been seen to contain two elements: a lighter staining peripheral region and a single, internal, dark-staining body (fig. 4). Incorporation of H^3-uridine occurs for the first time at this stage (Mintz, '64a). Nucleoli of 8-cell

embryos (fig. 5) and morulae (figs. 6, 7) differ from 4-cell nucleoli in that the internal nucleolar bodies are smaller and often stain less intensely than the peripheral region. A change in nucleolar form occurs at the blastocyst stage, where nucleoli are observed to be elongate and irregular in shape (fig. 8).

Electron microscopy

The spherical cytoplasmic vesicles (V), described previously, contain a medium-density substance and are not bounded by a unit membrane. In fact, nothing but an electron-dense line appears to maintain the integrity of the vesicle. Although coalescence of vesicles may occur, the commonly encountered picture where vesicles come in contact is one of vesicle integrity (fig. 9). In early developmental stages (1–8 cells) individual vesicles are commonly closely associated with one or more mitochondria (fig. 9). Such associations are less frequently observed in the morula stage.

Examination of adjacent thick sections and thin sections suggests that the dark-staining masses (C) observed with the light microscope correspond to crystalloids seen with the electron microscope. These crystalloids have been described by Enders and Schlafke ('65) as "aggregates of individual units about 40 mμ wide, 300 mμ long and with a cross-striation every 12 mμ" (fig. 10). No crystalloids are observed in unfertilized eggs, but in fertilized eggs small areas of crystalloid material are occasionally observed close to the nucleus (fig. 28). Small areas of crystalline material are present in the 2-cell embryo. From the 4-cell stage to the blastocyst, crystalloids increase in number and size. It is at the 8-cell stage that the crystalloids become visible as dark-staining masses with the light microscope. Crystalloid material at the morula stage (fig. 11) and the blastocyst stage is usually associated with rough endoplasmic reticulum, and strands continuous between crystalline material and the ribosomes of rough endoplasmic reticulum are occasionally seen (fig. 12).

A predominant type of cytoplasmic inclusion, observable only by electron microscopy, appears to consist of parallel arrays of straight or curved fibrous strands (fig. 14) exhibiting cross striations at 30 mμ intervals (Enders and Schlafke, '65). At high magnification (fig. 13) an individual strand is seen to consist of two long parallel strands (α), separated by a space of approximately 30 mμ. A third strand (β), appears to coil helically around both α strands, giving a periodicity of 30 mμ. This fibrous material was found in large amounts in all stages examined.

Structures are often observed which appear to consist of an inner sphere approximately 33 mμ in diameter surrounded by a larger sphere approximately 67 mμ in diameter, and which resemble "doughnuts" in cross-section. At the 4-cell stage (fig. 14) and 8-cell stage (fig. 15), large numbers of these "doughnuts" are seen within mitochondria-associated sacs. (Observations to be discussed below suggest that these sacs are endoplasmic reticulum, although few ribosomes are as yet attached to them.) Rarely, fine filaments can be seen projecting from the outer sphere of the "doughnut" toward the inner wall of the endoplasmic reticulum. In some sections it appears that the outer sphere has fused with the wall of the endoplasmic reticulum, while the inner sphere remains intact. At the morula stage "doughnuts" are only occasionally seen within the granular endoplasmic reticulum. From the 8-cell stage to the blastocyst, crystalloids are often associated with granular endoplasmic reticulum containing these "doughnuts."

Cytoplasmic ribosomes are identified as free (single) ribosomes, clusters of ribosomes (polysomes), and as components of the granular endoplasmic reticulum. There are very definite changes in these three classes of ribosomes as development progresses in the mouse.

Ribosomal clusters are seen in the unfertilized egg, the fertilized egg and the 2-cell stage. There is no rough endoplasmic reticulum detected at these early stages, no ribosomes along the outer membrane of the nuclear envelope and few free ribosomes. In the 4-cell embryo, clusters of ribosomes are observed in somewhat greater frequency than in earlier stages. Ribosomes are detected on the outer membrane of the nuclear envelope of the 4-cell stage and all later stages. Rough endoplasmic reticulum first appears at the 4-cell stage as small

mitochondria-associated sacs bearing a few ribosomes (figs. 14, 16). In the 8-cell embryo, free ribosomes are detected in very large numbers (fig. 15), although clusters of ribosomes and rough endoplasmic reticulum are also present. At the morula stage, ribosomes exist primarily in clusters or as components of granular endoplasmic reticulum; free ribosomes are rare. Blastocysts also possess many ribosomal clusters (fig. 21) and rough endoplasmic reticulum; the latter occasionally is continuous with the outer nuclear membrane.

At the 4-cell stage, clusters of ribosomes are detected along the periphery of the blastomeres, just beneath the cell membrane (fig. 17). Such clusters are also observed in 8-cell embryos (fig. 18). Ribosome clusters are occasionally seen close to the plasma membranes of adjacent peripheral cells of morulae (fig. 19), in regions where junctional complexes are observed in older morulae.

Obvious differences in the number or distribution of ribosomes in different cells, which might correspond to the differences in Azure B basophilia observed with the light microscope, were not evident in the morulae examined. However, in the blastocyst, differences in cytoplasmic background density are occasionally apparent between cells (fig. 21).

The Golgi apparatus does not seem to be a prominent feature in cells of preimplantation mouse embryos. Although large numbers of membranous sacs and vesicles are present throughout the cytoplasm, the typical aggregations of stacked cisternae and vesicles are rarely encountered. In all stages younger than the morula only small regions of stacked cisternae are occasionally observed. In the morula, larger regions of stacked cisternae are encountered and, rarely, continuity between Golgi material and rough endoplasmic reticulum can be seen (fig. 20). By the blastocyst stage fairly typical Golgi material is observed, usually in the vicinity of the nucleus.

Nearly all the mitochondria in murine preimplantation stages are of the vacuolated type described by Wischnitzer ('67) in the ovarian oocyte. In the unfertilized egg (fig. 22), fertilized egg and 2-cell stage, sectioned mitochondria have two forms: a nearly circular form, approximately 400 mμ in diameter, and an elongate form approximately 860 mμ by 400 mμ. (Larger mitochondria are occasionally encountered.) Assuming that mitochondria are oriented randomly, the similarity between the diameters of circular forms and the smaller diameters of elongate forms suggests that the mitochondria may be nearly cylindrical. The two forms would then be due to longitudinal or tangential sections (elongate forms) and cross-sections (circular forms). In 4-cell and older embryos, mitochondria are larger (600 mμ to 1,000 mμ in diameter) and are interpreted as being more spherical because elongate forms are rarely encountered. In most of the vacuolated mitochondria, fibrous strands, occasionally exhibiting a helical pattern, are observed within the intracristal vacuoles (fig. 23). Mitochondria are often contiguous to two types of organelles: "cytoplasmic vesicles," and "mitochondria-associated sacs" (endoplasmic reticulum).

Vesicle aggregates of a fairly distinct type are observed in preimplantation embryos and may be derived from multivesicular bodies, as suggested by Sotelo and Porter ('59) for similar aggregates observed in the rat ovum. These aggregates consist of membrane-bound vesicles of varying sizes exhibiting circular and cylindrical shapes. Some of the vesicles appear to contain other smaller bodies (fig. 24). Vesicle aggregates of this type seem to be more prevalent in the unfertilized egg, fertilized egg and 2-cell stage than in older stages and are usually located near the cell membrane. One distinctive type of body, often associated with these vesicle aggregates, is labelled (J) in figure 25. These bodies (J) are typically abutted against one another in a jigsaw pattern, but are also observed as single entities. Aggregates of "jigsaw bodies" correspond to the medium density areas (J) observed with the light microscope (fig. 1).

Another distinct type of body, observed in large numbers in the unfertilized and fertilized eggs, is a light-staining sac (S) with ill-defined margins (figs. 22, 23). These sacs contain light-density strands, and may be in association with mitochondria.

Cortical granules, consisting of an electron-dense body surrounded by a unit mem-

brane, are usually observed in the peripheral regions of unfertilized eggs. Rarely a more centrally located cortical granule is seen in the vicinity of Golgi material, which is reported to be the site of their formation in the rat (Szollosi, '67). Cortical granules were occasionally observed in the pronuclear stage, but not in any stages subsequent to the first cleavage division.

Microvilli are observed around the blastomeres in all preimplantation stages, and in favorable sections appear to possess a core of filaments similar to those reported by Palay and Karlin ('59) and McNabb and Sandborn ('64) in intestinal microvilli.

Few microvilli are found on the unfertilized egg or on the pronuclear fertilized egg, but they become numerous prior to the first cleavage and are present in all later preimplantation stages. At the 4-cell and 8-cell stages, there is some indication that microvilli begin to function in the adherence of blastomeres. In several regions where a microvillus comes near an adjoining cell, a close and constant distance is maintained between the villus and the cell (fig. 15). By the morula stage, microvilli also appear to function in the adherence of blastomeres by an interdigitation process in which the cell opposite a microvillus invaginates so that a lock-and-key fit is attained. This lock-and-key fit is also observed between cells of the blastocyst, particularly between trophoblast cells (fig. 26).

Specialized structures that appear to function in cellular adherence are not encountered until the morula stage, where "junctional complexes" or "tight junctions" are observed. Tight junctions are seen between peripheral cells of late morulae just below the free surface. These complexes consist of an amorphous dense substance located in the intercellular space and extending across the cell membranes into the cytoplasm of both cells. This dense substance extends over a considerable length of attachment for the most peripheral (presumptive trophoblast) cells (fig. 27). Tight junctions are also present in the blastocyst, where they are found between the trophoblast cells which are adjacent to the inner cell mass (fig. 26), and between trophoblast cells bordering the blastocoel.

Nucleoli undergo several changes in appearance during preimplantation development. After fertilization, spherical agranular "nucleoli," composed primarily of fine fibrils, appear in the pronuclei (fig. 28). A small area of condensed chromatin is often seen in close proximity to these "nucleoli." "Tertiary nucleoli" as described by Szollosi ('65) in pronuclei of the rat were not seen, although the membrane bound extrusion bodies of fig. 29 may be similar to them. Smooth, spherical "nucleoli" are also found in the 2-cell stage. At the 4-cell stage, a net-like nucleolonema containing fibrils and granules is observed around the periphery of large agranular spherical bodies. The nucleolonema is reported by Bernhard ('65) to consist of a protein matrix with RNA-containing fibrils and ribonucleoprotein granules embedded within it . The nucleoli of the 8-cell stage (fig. 30) are very similar to 4-cell stage nucleoli, but contain a larger nucleolonema. The nucleoli of morulae exhibit the two structural elements typically observed in nucleoli (Fawcett, '66): a net-like nucleolonema and several spherical dense areas, the partes amorphae. The partes amorphae are similar in structure to the spherical agranular "nucleoli" of the fertilized egg and 2-cell stage and to the large agranular central body of 4-cell and 8-cell stage nucleoli. In the early blastocyst, nucleoli generally appear similar to those observed in morulae (fig. 31), but in older blastulae, nucleolar shape changes to a more elongate and irregular form. The partes amorphae are smaller and less dense in blastocyst nucleoli (fig. 31).

Elaborate intranuclear annulate lamellae (IAL) are seen in fertilized egg pronuclei (fig. 28) and in 2-cell stage nuclei. Shorter IAL segments are routinely observed in nuclei of 4-cell, 8-cell and morula stages and occasionally in blastocyst nuclei. The structure of these intranuclear annulate lamellae has been described in another paper (Calarco and Brown, '68). In general, IAL resemble the nuclear envelope, are usually oriented perpendicularly to it, and occasionally are observed to be continuous with the inner membrane of the nuclear envelope. Pores and sac-like dilations are often evident along the IAL. The IAL observed in this study resemble

the IAL of other species described by Kessel ('68). After the second cleavage, IAL are typically observed in association with chromatin or nucleolar material.

Nuclear pores are a regular feature of the nuclear envelope in blastomeres of all cleavage stages examined.

DISCUSSION

A number of investigators have reported evidence of differentiation in rodent preimplantation stages. Mulnard ('65) reported a differential reaction of the inner cell mass for acid phosphatase activity in the morula stage: the cells of the inner cell mass stain intensely ("diffuse reaction") and the surrounding cells stain weakly ("granular reaction"). Smith ('56) reported that blastocysts exhibit a layer of trophoblast cells which stain more intensely with the PAS technique than do the cells of the inner cell mass. According to Enders and Schlafke ('65), the first ultrastructural differences *between* cells are seen in the late blastocyst stage, when endoderm cells exhibit an increase in the amount and dilation of the endoplasmic reticulum. Baevsky ('61) also reported the earliest cytological indication of differentiation in the rat to be the differentiation into ectoderm and endoderm of the inner cell mass of the late blastocyst.

In the present study, differences in cytoplasmic basophilia (Azure B staining) were observed *between* different cells of some morulae. Differences were also seen between trophoblast cells (more densely stained) and cells of the inner cell mass of blastocysts. At the fine structural level, no obvious differences in numbers or distributions of organelles, which might indicate differentiation, were observed between the blastomeres of any particular preimplantation stage. Electron micrographs of early blastulae, however, revealed differences in cytoplasmic background density between some cells. The lack of ultrastructural differentiation prior to the blastocyst stage may be related to the regulative ability of cleavage stages. The differences in Azure B basophilia between cells observed within late morulae and blastocysts, and the differences in background density observed ultrastructurally in blastocysts, might be related to an early stage of differentiation, reflected in differing rates of protein synthesis. The regulative ability of blastocyst cells has not been examined, but it is possible that the observed differences in cytoplasmic basophilia within blastocysts reflect a change in the determination of cells at this time. Alternatively, the differential basophilia may simply be due to differences in cell volumes or asynchronous cell cycles.

Crystalloid inclusions have often been interpreted as storage forms of proteins synthesized within cells (Fawcett, '66). The crystalloids observed in preimplantation stages of the mouse may correspond to the "dark yolk" observed by Lewis and Wright ('35). Crystalloids were not observed in this study in the unfertilized egg, but increased in amount from fertilization to the blastocyst stage. Crystalloids, therefore, do not represent a "yolk" product used up in early development. In fact, the preimplantatian embryo, which contains little food reserves, not only meets the energy requirements of cleavage and blastulation but also synthesizes these crystalloids. The frequent association of the crystalloids with endoplasmic reticulum, particularly the occasional observation of strands of the crystalloids in contact with the membrane-bound ribosomes, suggests that the crystalloids are proteinaceous. In embryos homozygous for the t^{12} mutation, which die at the morula stage, incomplete crystalloid-like aggregates are surrounded by free ribosomes (Calarco and Brown, '68). Since t^{12}/t^{12} embryos contain large numbers of free ribosomes, but few ribosome clusters, they may be defective in protein synthesis. This could explain the presence of apparently incomplete crystalloid-like aggregates. The function of these crystalloids is not known; they may represent a product synthesized during preimplantation stages and utilized by the cells later in development.

The relative abundance of the fibrous material has been reported to diminish from early cleavage to the blastocyst stage (Enders and Schlafke, '65). Noticeable decreases in amounts of the fibrous material during cleavage were not observed in this study, however. Although the function of this fibrous material is unknown, Szollosi

('65) has described the accumulation of similar material in growing ovarian oocytes of the rat and hamster and suggests that it represents a yolky substance.

Enders and Schlafke ('65) detected a "virus-like particle" within the endoplasmic reticulum of guinea pigs in the 8-cell stage and later stages of development. In their figure 4, a "sphere within a sphere" substructure is clearly seen. The substructure of the "doughnuts" observed in this study, and their location within endoplasmic reticulum sacs, suggests that they, too, may be viruses. Their size range would probably place them in the group of viruses termed adenoviruses. If these "doughnuts" are viruses, the interpretation of the observed increase in crystalloids subsequent to fertilization, and speculations regarding the function of the crystalloids, become even more difficult, since certain viruses are known to aggregate in crystalline arrays (Breese and Graves, '67). If these entities could be identified as viruses, the presumably tolerant cleavage stages would be a favorable system in which to study their ontogeny. "Doughnuts" were present in all embryos subsequent to the 2-cell stage examined ultrastructurally in this study, which suggests that they are normally present in the preimplantation stages of mice from this colony. It is worth noting that there appeared to be no unusual differences in litter size, fertility or life span of mice from this colony.

The appearance of large numbers of free ribosomes at the 8-cell stage, followed in the morula stage by the appearance of many ribosomal clusters, suggests that clustering occurs after ribosome synthesis, probably as a result of the attachment of ribosomes to messenger RNA. The observation that ribosome clustering normally begins subsequent to the 8-cell stage, suggests that embryos homozygous for the t^{12} mutation, which may attain 30 cells (Smith, '56) and yet contain few ribosomal clusters (Calarco and Brown, '68), do not progress "developmentally" past the normal 8-cell stage, even though cleavage continues for a time.

It was reported by Mintz ('62) that blastomeres of the 2-cell stage often do not adhere well to one another when the zona pellucida is removed; this was not found to be true of the cells of older stages, which she reported as being "sticky" (at 37° C). In the present study, ribosomes were frequently observed adjacent to the plasma membrane of blastomeres from the 4-cell stage through the 8-cell stage. In the morula, ribosomes were present along cell-cell boundaries only in the regions of the cells near the periphery of the embryo; older morulae possess junctional complexes in these regions. A reasonable assumption is that these ribosomes are involved either in the synthesis of structural components of the plasma membrane or in the synthesis of a proteinaceous component of a material responsible for the adhesiveness of blastomeres and the formation of junctional complexes. Consistent with this suggestion is the observation that the blastomeres of embryos homozygous for the t^{12} mutation, which may be defective in protein synthesis (as discussed previously), adhere less well to one another than do normal blastomeres (Calarco and Brown, '68).

Prior to the 4-cell stage the endoplasmic reticulum seems to exist in a nascent form as mitochondria-associated sacs, which later become granule encrusted. By the morula stage, continuity between endoplasmic reticulum and the outer nuclear membrane is occasionally observed, suggesting that additional endoplasmic reticulum elaborated later in development may be formed from the outer nuclear membrane. Typical smooth endoplasmic reticulum was not observed in any preimplantation stages.

Thompson and Brinster ('66) reported large amounts of glycogen (PAS-positive, diastase-removable material), in preimplantation mice from the 2-cell to the morula stages. Stern and Biggers ('68), utilizing enzymatic techniques for ultramicro determinations of glycogen, reported a value of 0.14 mμg glycogen in the fertilized egg, which rose to a peak of 2.24 mμg glycogen/embryo at the 8-cell stage and declined to 1.81 mμg glycogen/embryo at the blastocyst. The usual ultrastructural appearance of glycogen, in sections in which lead has been used to enhance contrast, is that of very electron-dense clusters composed of individual β particles which are 150–300 Å in diameter (Fawcett, '66).

No typical glycogen clusters were observed in any preimplantation stages examined in this study. There are several possible explanations for the difference tween the biochemical and ultrastructural observations:

1. Glycogen in preimplantation embryos may exist primarily in the form of non-clustered β particles which can occasionally be confused with single ribosomes. Thus, β particles of glycogen could comprise part of the class of particles which we have designated "free ribosomes" (fig. 15). Two observations argue against the presence of non-clustered β particles and thus against the confusion of such particles and ribosomes. (1) Although there is a 10-fold increase in glycogen from the fertilized egg to the 2-cell stage (see table 2 in Stern and Biggers, '68), we did not observe a corresponding increase in the population of cytoplasmic "particles." (2) Although Stern and Biggers found that the amount of biochemically-detected glycogen at the 8-cell stage (2.24 mμg/embryo) is nearly the same at the 16-cell (morula) stage (2.17 mμg/embryo), we observed very few free "ribosomes" in morulae. Instead, morulae exhibit clusters of medium-density particles, which we interpret to be polysomes; clustered β particles of glycogen are typically very electron dense.

2. The amount of glycogen present in preimplantation embryos does not correspond to a large enough population of β particles to be detected with the electron microscope. To our knowledge the exact particle weight of a β particle of glycogen is not known. However, if particle weights are assumed to vary from a small average textbook value of 1×10^6, to the large 180×10^6 weight average molecular weight of glycogen in *Ascaris* (Orrell et al., '64), and using the value of 2.24 mμg of glycogen present in an 8-cell embryo, one would expect from 400,000 to 2,000 glycogen β particles to be within our average section of a blastomere at the 8-cell stage, presumably enough to be noticed.

3. Glycogen is so localized subcellularly that it was not detected due to the sampling error introduced by ultrastructural observations.

4. Glycogen exists in a form other than the standardly recognized clusters of β particles, most probably a soluble form.

Brinster ('65a, '67) concluded from investigations on the energy sources necessary for murine preimplantation development that at the 8-cell stage a deamination enzyme becomes available, and probably a new metabolic pathway is being used. The increase in mitochondrial size and the change in shape to a more spherical form, observed first at the 4-cell stage, may be correlated with the metabolic changes reported by Brinster.

Vacuolated mitochondria were noted by Yamada et al., ('57) in the mouse ovarian oocyte, and Wischnitzer ('67) traced the development of this type of mitochondrion in mouse ovarian oocytes. Wischnitzer reported that the vacuoles arise from the dilation of an intracristal space which enlarges and eventually pushes the other cristae against the inner mitochondrial membrane. Observations on preimplantation embryos in the present study also suggest that the intramitochondrial vacuoles are enlargements of one or more intracristal spaces. The different fixation procedures used in the initial phases of this study (Calarco, '68) consistently revealed intramitochondrial vacuoles in embryonic material but not in other cells fixed in the same manner, most notably cumulus cells still adhering to the unfertilized egg.

Wischnitzer ('67) suggested that transformation of oocyte mitochondria to the vacuolated type "reflects the response of the cells to unusual physiological needs during maturation and differentiation." The present study reveals that vacuolated mitochondria exist as the dominant mitochondrial form at least until implantation. Assuming that there is a correlation between mitochondrial internal structure and function, the continued presence of the altered mitochondria reflects more than the physiological needs of the oocyte. One might speculate that the frequent association of vacuolated mitochondria with cytoplasmic vesicles is in some way related to mitochondrial function. On the other hand the altered mitochondrial morphology may simply be due to differences in permeability of the embryo to the fixatives.

The spherical lipid-like inclusions which are numerous in preimplantation embryos have been referred to as "cytoplasmic vesicles" in this study in order to call attention to their proposed role in blastocoel formation. These vesicles presumably correspond to the "light yolk globules" observed by Lewis and Wright ('35) and the "spherical bodies" observed by Mintz ('64a). One suggestion exists (Melissinos, '07) that "intracellular globules" contain blastocoel fluid which is secreted to form the blastocoel.

Several observations in the present study support the notion that the cytoplasmic vesicles are involved in blastocoel formation. (1) The number of cytoplasmic vesicles increases up to the 4-cell stage. (2) Subsequent to the 4-cell stage, the size of the vesicles increases as their number decreases. (3) The vesicles are often localized near intercellular margins. (4) Few cytoplasmic vesicles are present in the cells of the blastocyst.

The observed decrease in vesicle number subsequent to the 4-cell stage could be due to coalescence of vesicles resulting in fewer, but larger vesicles. A decrease in vesicle number would also result if some "dumping" of vesicle contents into intercellular spaces occurs subsequent to the 4-cell stage. Possibly both of these occurrences lead to the observed decrease in the number of vesicles. It is worth noting that Dalcq ('55) has suggested that blastulation in rodents may begin between the 8-cell and morula stages.

Continuity between cytoplasmic vesicle boundaries and the cell membrane was not observed with the electron microscope. Such an association between the unit membrane of the cell and the non-membrane-bound vesicles would presumably be difficult to detect. However, vesicles are often seen close to intercellular boundaries subsequent to the 4-cell stage. Figure 32 may represent a stage just prior to the dumping of the cytoplasmic vesicle contents into the intercellular space.

What is the origin of the cytoplasmic vesicles and their contents? Very few pinocytotic invaginations or vesicles (pinosomes) were observed in this study, suggesting that pinocytosis is not an important process for providing vesicle contents. In the unfertilized egg, large numbers of light-staining sacs (S) with ill-defined margins are observed, some in association with mitochondria (fig. 33). These sacs contain several light-staining strands. Perhaps mitochondria associate with these sacs and act upon them in some way, changing them into the recognized form of cytoplasmic vesicles. However, no definitive answer to the question of cytoplasmic vesicle origin can be obtained from the ultrastructural information available.

Observations made on the nucleolus indicate that a change in form occurs at the 4-cell stage. The nucleolonema, containing granular and fibrillar portions, appears around a large agranular body which is similar in structure to the smooth "nucleoli" of younger stages. It is at the 4-cell stage that nucleoli first incorporate H^3-uridine (Mintz, '64a). These observations suggest that the onset of nucleolar function is associated with the appearance of the nucleolonema. Similar changes in nucleolar ultrastructure correlated with the onset of nucleolar function, i.e., synthesis of ribosomal RNA, have been reported for *Triturus* (Karasaki, '65), and for the rat (Szollosi, '66).

Moses ('60) reported that the nuclear envelope in a variety of organisms reforms after cell division by the adherence of vesicular components resembling endoplasmic reticulum to the chromosomes, and the subsequent fusion of these vesicles into flattened cisternae which eventually form a continuous nuclear envelope. "Pores" are not evident in cytoplasmic endoplasmic reticulum, but are found in endoplasmic reticulum after its adherence to chromosomes. It is possible that the intranuclear annulate lamellae observed in this study represent remnants of endoplasmic reticulum which were not incorporated into the nuclear envelope but were trapped inside it. However, if IAL are simply remnants of endoplasmic reticulum, one might expect to find them in roughly the same frequency in all developmental stages. This is not the case. IAL appear in large numbers in the pronuclear and 2-cell stages and in decreasing amounts in progressively later stages.

CONCLUSIONS

Preimplantation development in the mouse is marked by the appearance and elaboration of several cellular organelles, inclusions and cell surface specializations.

During the 24 hours from sperm contact to the first cleavage, the 1-cell embryo develops pronuclei which contain many intranuclear annulate lamellae (IAL) and several spherical dense "nucleoli." The number of cytoplasmic vesicles (V) increases and crystalloids are detected in small amounts for the first time. Mitochondria are primarily cylindrical, vacuolated and similar to those of the unfertilized egg. Prior to the first cleavage, numerous microvilli are elaborated.

In the interval (approximately 12 hours) that the 2-cell stage exists, the cellular organelles and inclusions undergo little change except for an increase in the number of cytoplasmic vesicles.

The 4-cell stage lasts approximately 12 hours, during which time there are many changes. A functional nucleolus, characterized ultrastructurally by the presence of a net-like nucleolonema, appears. IAL are present in smaller amounts than in the 2-cell embryo. Cytoplasmic vesicles reach a peak numerically and are often observed near intercellular margins. Crystalloids are present in greater amounts than previously. Many ribosomes are found near the periphery of the blastomeres and the adherence of adjacent cells begins. Small amounts of rough endoplasmic reticulum are detected as mitochondria-associated sacs bearing a few ribosomes. Vacuolated mitochondria increase in size and change from the cylindrical form, present in younger embryos, to a more spherical form.

The 8-cell stage is marked by the further elaboration of the organelles and inclusions characteristic of the 4-cell stage. In addition, large numbers of free ribosomes are present and cytoplasmic vesicles have increased in size and decreased in number.

Cells of the morula exhibit a typical nucleolus. IAL are often observed in association with chromatin or nucleolar material. The early morula exhibits ribosomes along peripheral cell-cell boundaries, while the late morula possesses junctional complexes in these regions. Cell adherence is also aided by the interdigitation of microvilli. Cytoplasmic vesicles often appear fewer in number, especially in peripheral cells, and intercellular spaces are occasionally enlarged. Crystalloids are numerous and are usually associated with rough endoplasmic reticulum. Ribosomes exists predominantly in clusters, presumably polysomes. Individual late morulae also exhibit differences in cytoplasmic basophilia *between* cells, which may be a prelude to differentiation.

It is suggested that the contents of the blastocoel are derived from cytoplasmic vesicles which increase in number subsequent to fertilization and then decrease in number as they coalesce and release their contents into intercellular spaces. The blastocoel arises as these fluid-filled spaces become confluent and enlarge. During the blastocyst stage, nucleoli change to an elongate irregular form. Cytoplasmic vesicles are few in number, often quite large, and are located near enlarged intercellular spaces in young blastocysts. Differences in cytoplasmic background density can now be observed between cells of the blastocyst but there are no observable differences in the amounts or the locations of organelles. The blastocyst stage marks the end of the preimplantation development of the mouse.

ACKNOWLEDGMENTS

The authors wish to gratefully acknowledge the helpful criticisms of this manuscript provided by Dr. Daniel Szollosi.

LITERATURE CITED

Baevsky, U. B. 1961 Some observations on changes in blastocysts during lactation diapause in albino rats. J. Anat. Histol. Embryol., *41:* 14–18.

Bernhard, W. 1965 Ultrastructural aspects of the normal and pathological nucleolus in mammalian cells. In: International Symposium on the Nucleolus—Its Structure and Function. W. S. Vincent and O. L. Miller, eds. National Cancer Institute Monograph No. 23, U.S. Government Printing Office, Washington, D.C., pp 13–28.

Breese, S. S., and J. H. Graves 1967 Crystalline arrays of foot-and-mouth disease virus in tissue culture cells. Proceedings of the Electron Microscopic Society of America, 25: 102–103.

Brinster, R. L. 1965a Studies of the development of mouse embryos *in vitro:* energy metabolism. In: Preimplantation Stages of Pregnancy. G. E. W. Wolstenholme and M. O'Connor, eds. Little Brown and Co., Boston, pp. 60–74.

——— 1965b Studies on the development of mouse embryos *in vitro*. I. The effect of osmolarity and hydrogen ion concentration. J. Exp. Zool., *158:* 49–58.

——— 1967 Carbon dioxide production from lactate and pyruvate by the preimplantation mouse embryo. Exptl. Cell Res., *47:* 634–637.

Calarco, P. G. 1968 Cytological and ultrastructural observations of t^{12}/t^{12} and normal preimplantation stages of the mouse, *Mus musculus*. Ph.D. Thesis, University of Illinois, 111 pages.

Calarco, P. G., and E. H. Brown 1968 Cytological and ultrastructural comparisons of t^{12}/t^{12} and normal mouse morulae. J. Exp. Zool., *168:* 169–186.

Dalcq, A. M. 1955 Processes of synthesis during early development of rodents' eggs and embryos. Proc. Soc. Study Fert., *7:* 113–122.

Edwards, R. G., and A. H. Gates 1959 Timing of the stages of the maturation divisions, ovulation, fertilization and the first cleavage of eggs of adult mice treated with gonadotropins. J. Endocrin., *18:* 292–304.

Ellem, K. A. O., and R. B. L. Gwatkin 1968 Patterns of nucleic acid synthesis in the early mouse embryo. Develop. Biol., *18:* 311–330.

Enders, A. C., and S. J. Schlafke 1965 The fine structure of the blastocyst: some comparative studies. In: Preimplantation Stages of Pregnancy. G. E. W. Wolstenholme and M. O'Connor, eds. Little Brown and Co., Boston, pp 29–54.

Fawcett, D. W. 1966 The Cell. W. B. Saunders, Co., Philadelphia. 448 pages.

Flax, M. H. 1953 Ribose nucleic acid and protein during oogenesis and early embryonic development in the mouse. Ph.D. Thesis, Columbia University, 41 pages.

Huber, G. C. 1915 The development of the albino rat, *Mus norvegicus albinus*. I. From the pronuclear stage to the stage of mesoderm anlage. J. Morph., *26:* 247–358.

Izquierdo, L. 1967 A microchamber for processing mammalian eggs. Stain Tech., *42:* 35–37.

Izquierdo, L., and J. D. Vial 1962 Electron microscope observations on the early development of the rat. Zeit. für Zellforsch., *56:* 157–179.

Karasaki, S. 1965 Electron microscopic examination of the sites of nuclear RNA synthesis during amphibian embryogenesis. J. Cell Biol., *26:* 937–958.

Kessel, R. G. 1968 Annulate lamelle. J. Ultrastruct. Res., Suppl. *10:* 1-82.

Lewis, W. H., and E. S. Wright 1935 On the early development of the mouse egg. Carneg. Inst. Contrib. to Embryol., *25:* 115–143.

Luft, J. H. 1961 Improvements in epoxy resin embedding methods. J. Biophys. Biochem. Cytol., *9:* 409–414.

McNabb, J. D., and E. Sandborn 1964 Filaments in the microvillous border of intestinal cells. J. Cell Biol., *22:* 701–704.

Maser, M. D., T. E. Powell and C. W. Philpott 1967 Relationships among pH, osmolality, and concentration of fixative solutions. Stain Tech., *42:* 175–182.

Mazanec, K. 1965 Submikroskopische Veränderungen während der Furchung eines Säugetiereies. Arch. Biol., *76:* 49–85.

Mazanec, K., and M. Dvorak 1964 On the submicroscopical changes of the segmenting ovum in the albino rat. Cslka. Morfologie, *2:* 103–108.

Melissinos, K. 1907 Die Entwicklung des Eies der Mäuse. Arch. f. mikr. Anat., *70:* 577–628.

Mintz, B. 1962 Experimental study of the developing mammalian egg: removal of the zona pellucida. Science, *133:* 594–595.

——— 1964a Synthetic processes and early development in the mammalian egg. J. Exp. Zool., *157:* 85–100.

——— 1964b Gene expression in the morula stage of mouse embryos as observed during development of t^{12}/t^{12} lethal mutants *in vitro*. J. Exp. Zool., *157:* 267–272.

——— 1964c Formation of genetically mosaic mouse embryos and early development of "lethal (t^{12}/t^{12}) normal" mosaics. J. Exp. Zool., *157:* 273–292.

Monesi, V., and V. Salfi 1967 Macromolecular synthesis during early development in the mouse embryo. Exptl. Cell Res., *46:* 632–635.

Moses, M. J. 1960 Breakdown and reformation of the nuclear envelope at cell division. In: Proc. of the 4th Internat. Conf. on Electron Microscopy. Springer-Verlag, Berlin, pp. 230–233.

Mulnard, J. G. 1965 Studies of regulation of mouse ova *in vitro*. In: Preimplantation Stages of Pregnancy. G. E. W. Wolstenholme and M. O'Connor, eds. Little Brown and Co., Boston, pp. 123–138.

Orrell, S. A. Jr., E. Bueding and M. Reissig 1964 Physical characteristics of undegraded glycogen. In: Control of Glycogen Metabolism. W. J. Whelan and M. P. Cameron, eds. Little Brown and Co., Boston, pp. 29–52.

Palay, S. L., and L. J. Karlin 1959 An electron microscopic study of the intestinal villus. I. The fasting animal. J. Biophys. Biochem. Cytol., *5:* 363–372.

Reynolds, E. S. 1963 The use of lead citrate at high pH as an electron-opaque stain in electron microscopy. J. Cell Biol., *17:* 208–212.

Schlafke, S., and A. C. Enders 1963 Observations on the fine structure of the rat blastocyst. J. Anat., *97:* 353–360.

Smith, L. J. 1956 A morphological and histochemical investigation of a preimplantation lethal (t^{12}) in the house mouse. J. Exp. Zool., *132:* 51–83.

Snell, G. D., and L. C. Stevens 1966 Early embryology. In: Biology of the Laboratory Mouse. McGraw Hill, New York, pp. 205–246.

Sobotta, J. 1895 Die Befruchtung und Furchung des Eies der Maus. Arch. f. mikr. Anat., *45:* 15–93.

Sotelo, J. R., and K. R. Porter 1959 An electron microscope study of the rat ovum. J. Biophys., Biochem. Cytol., *5:* 327–342.

Stern, S., and J. D. Biggers 1968 Enzymatic estimation of glycogen in the cleaving mouse embryo. J. Exp. Zool., *168:* 61–67.

Szollosi, D. 1965 Extrusion of nucleoli from pronuclei of the rat. J. Cell Biol., *25:* 545–562.

——— 1965 Development of "yolky substance" in some rodent eggs. Anat. Rec., *151:* 424.

——— 1966 Nucleolar transformation and ribosome development during embryogenesis of the rat. J. Cell Biol., *31:* 115A.

——— 1967 Development of cortical granules and the cortical reaction in rat and hamster eggs. Anat. Rec., *159:* 431–446.

Thompson, J. L., and R. L. Brinster 1966 Glycogen content of preimplantation mouse embryos. Anat. Rec., *155:* 97–102.

Watson, M. 1958 Staining of tissue sections for electron microscopy with heavy metals. J. Biophys. Biochem. Cytol., *4:* 475–478.

Wischnitzer, S. 1967 Intramitochondrial transformations during oocyte maturation in the mouse. J. Morph., *121:* 29–46.

Yamada, E., T. Muta, A. Motomura and H. Koga 1957 The fine structure of the oocyte in the mouse ovary studied with electron microscope. Kurume Med. F., *4:* 148–171.

PLATE 1

EXPLANATION OF FIGURES

Phase contrast photomicrographs of 2 μ sections through BALB/c developmental stages fixed in glutaraldehyde, postfixed in osmium tetroxide and embedded in EPON. The sections were stained with Azur B bromide.

1 Unfertilized egg. V, cytoplasmic vesicles; Ch, chromosomes; J, medium density areas. × 750.

2 Fertilized egg. Note the two pronuclei, containing nucleoli (N), and the cytoplasmic vesicles (V). × 750.

3 Two-cell stage. The nucleus contains a number of spherical nucleoli (N). Cytoplasmic vesicles (V) are present and the zona pellucida (Z) is visible. × 750.

4 Four-cell stage. The nucleolus (N) now consists of two elements: a darker-staining central body and a lighter-staining peripheral region. V, cytoplasmic vesicles. × 750.

5 Eight-cell stage. V, cytoplasmic vesicles; N, nucleoli. × 750.

6 An embryo of approximately 15 cells. Note the slightly enlarged intercellular spaces and the lighter-staining central portion of the nucleolus (N). C, crystalloids; V, cytoplasmic vesicles. × 750.

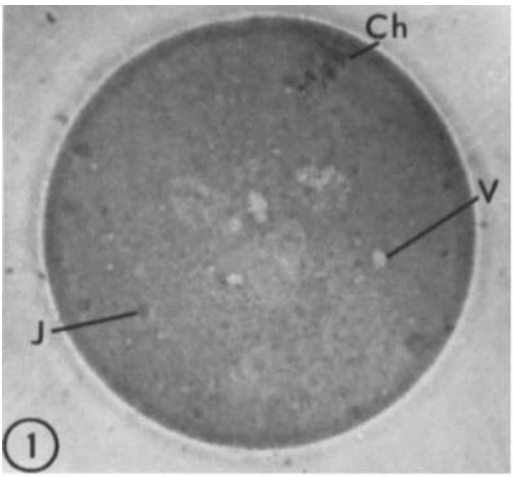
Ch
V
J
1

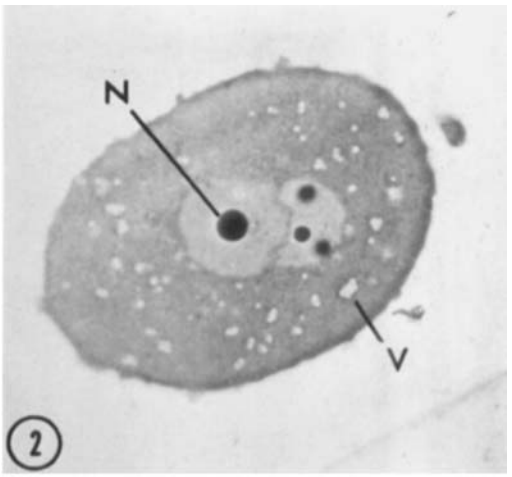
N
V
2

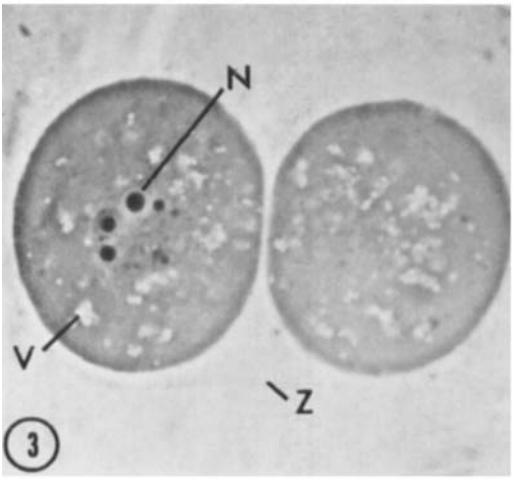
N
V
Z
3

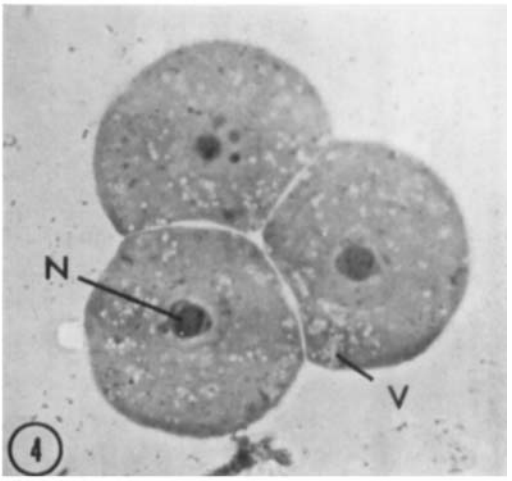
N
V
4

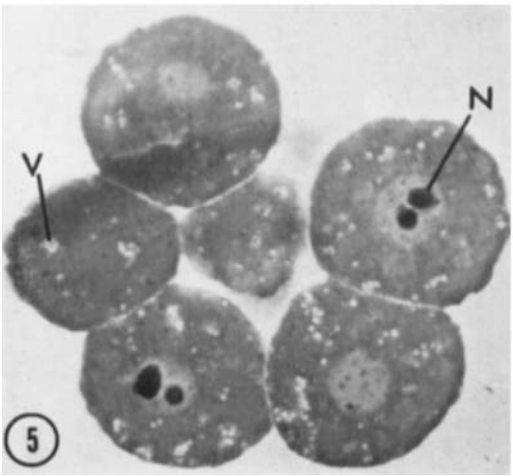
V
N
5

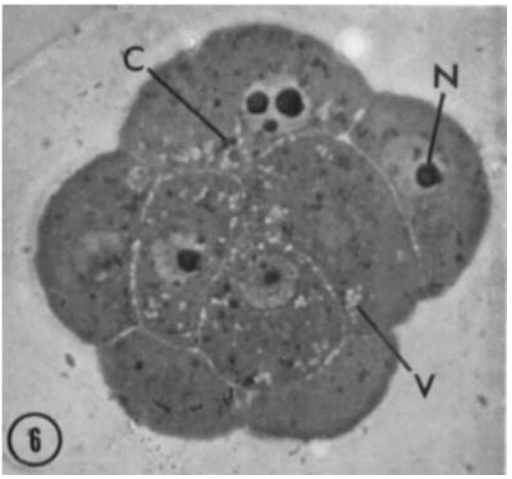
C
N
V
6

PLATE 2

EXPLANATION OF FIGURES

7 Photomicrograph of a 2 μ section through a morula. Note the differences in staining between different blastomeres. V, cytoplasmic vesicles; N, nucleolus. × 750.

8 A 2 μ section through a blastocyst. V, large cytoplasmic vesicles; N, an elongate nucleolus; Z, the zona pellucida. × 750.

9 Electron micrograph of a section through a blastomere of a 2-cell stage BALB/c embryo. Note the vacuolated mitochondria (M), their association with the lipid-like cytoplasmic vesicles (V), and the exaggerated pattern where the vesicles come in contact. C, crystalloids; F, fibrous material. × 30,150.

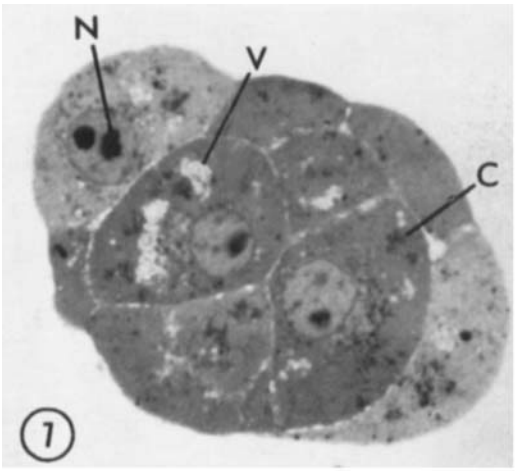
N
V
C
7

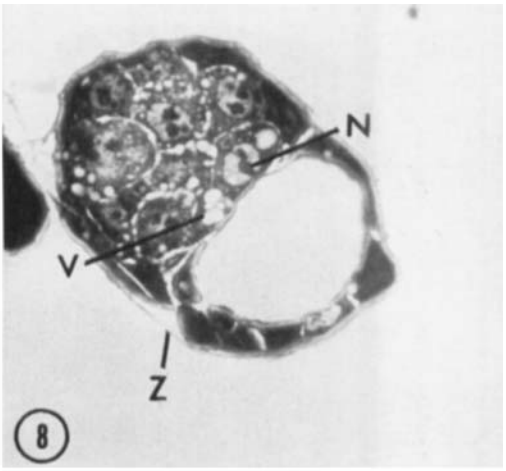
N
V
Z
8

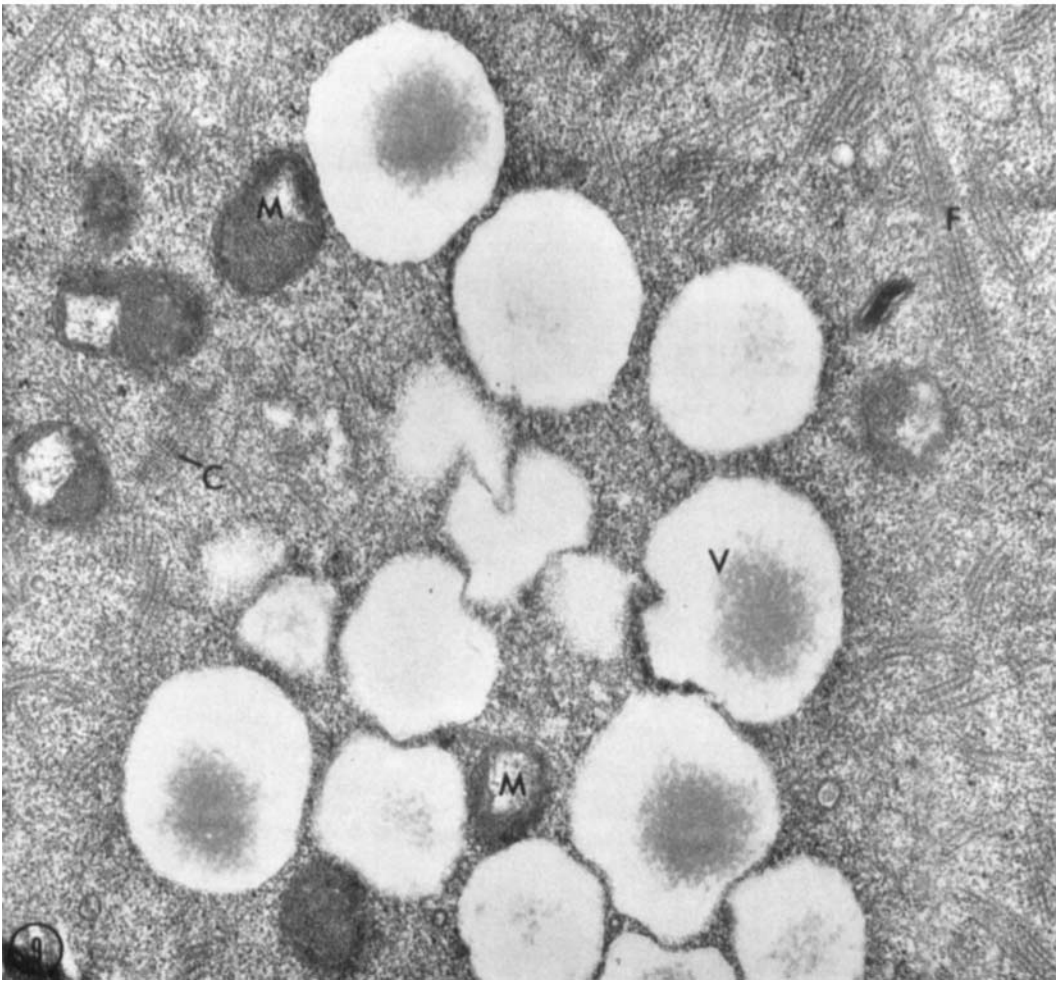
M
F
C
V
M
9

PLATE 3

EXPLANATION OF FIGURES

10 Typical crystalloids (C) in a morula. × 60,300.

11 Morula stage. Crystalloids (C) associated with granular endoplasmic reticulum (ER) and "doughnuts" (D). × 30,150.

12 The arrow indicates fibrous strands which appear to extend from two ribosomes (attached to a mitochondria-associated sac, i.e. endoplasmic reticulum) into a crystalloid area (C). M, mitochondrion. × 60,300.

13 Typical fibrous material in a 4-cell stage. The fibrous array appears to consist of subunits, each composed of a strand (β) which appears to coil helically around two parallel strands (α). × 60,300.

14 Large numbers of structures (D), resembling "doughnuts" in cross section, are seen within sacs in this 4-cell embryo. Note the closely associated crystalloids (C). The arrow indicates a mitochondria-associated sac bearing 2 ribosomes and interpreted as being endoplasmic reticulum. M, mitochondrion. × 30,150.

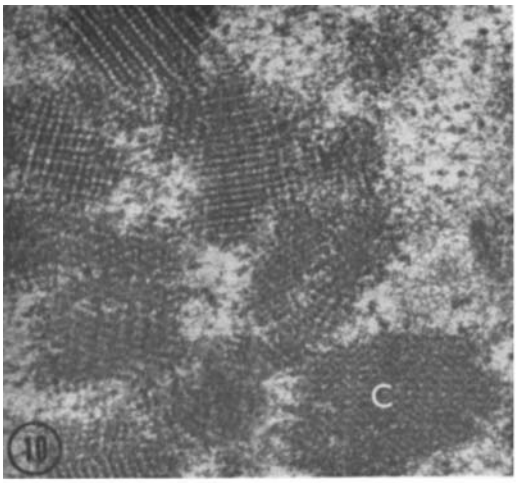
C
10

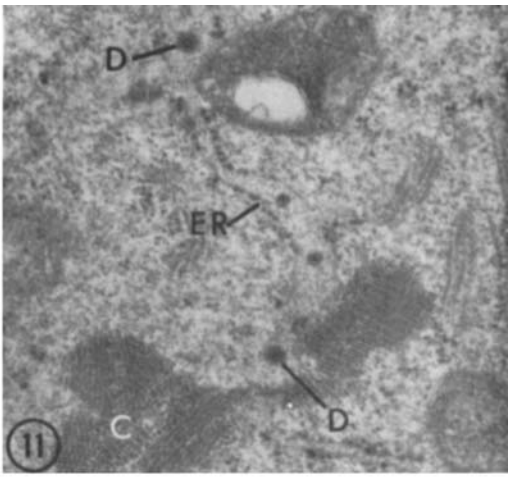
D
ER
C
D
11

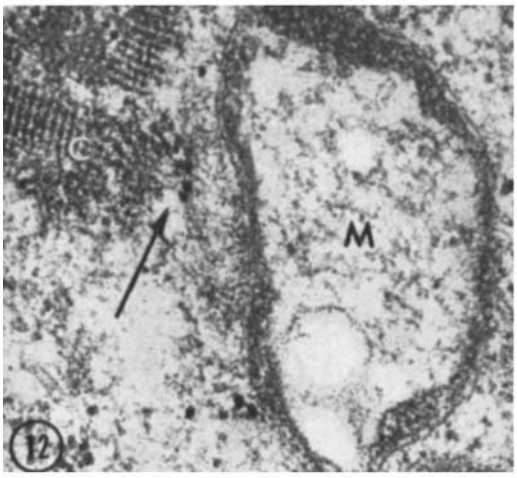
C
M
12

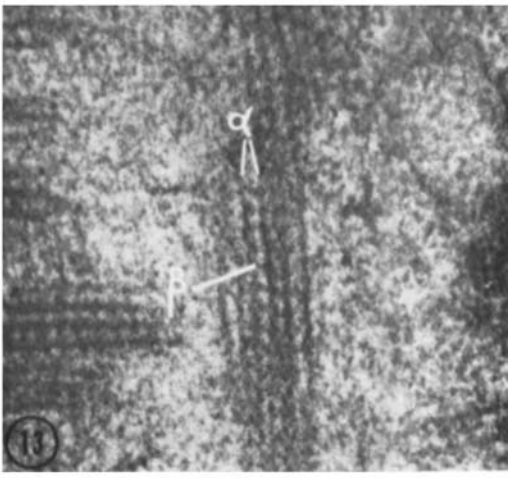
A
P
13

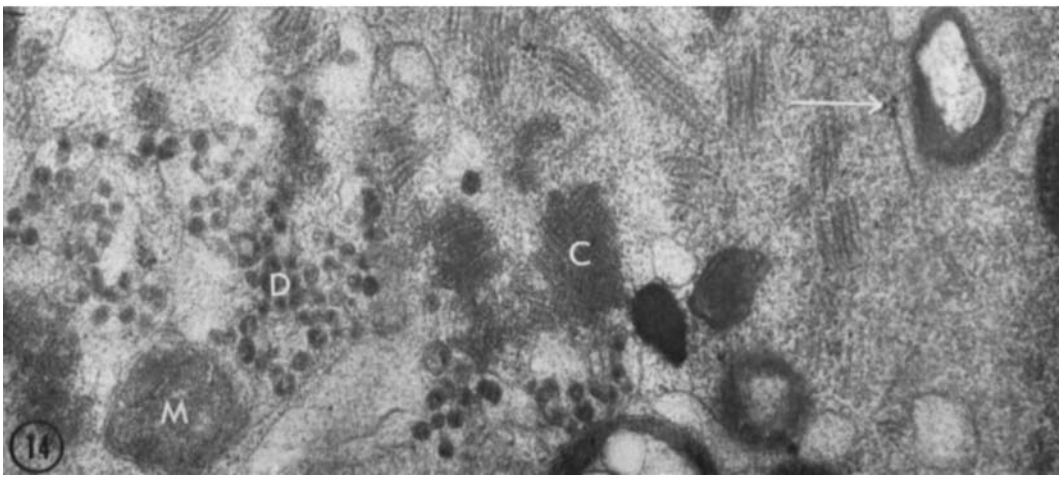
C
D
M
14

PLATE 4

EXPLANATION OF FIGURES

15 Large numbers of free "ribosomes" are visible in this blastomere of an 8-cell embryo. Note that these free particles are smaller in size than those in the cluster within the square at the top of the micrograph. D, "doughnuts"; G, Golgi material; M, mitochondrion; C, crystalloids; X, an area of close apposition of two blastomeres; arrow, a mitochondria-associated sac. × 30,150.

16 Cytoplasmic vesicle (V) near an intercellular space of a 4-cell embryo. The arrow indicates a mitochondria-associated sac bearing a few ribosomes and interpreted as being rough endoplasmic reticulum. M, mitochondrion; X, a region of close association between a microvillus and an adjacent blastomere. × 30,150.

17 Ribosomal clusters (R) are localized along the periphery of this blastomere from a 4-cell stage. M, mitochondrion; F, fibrous material. × 30,150.

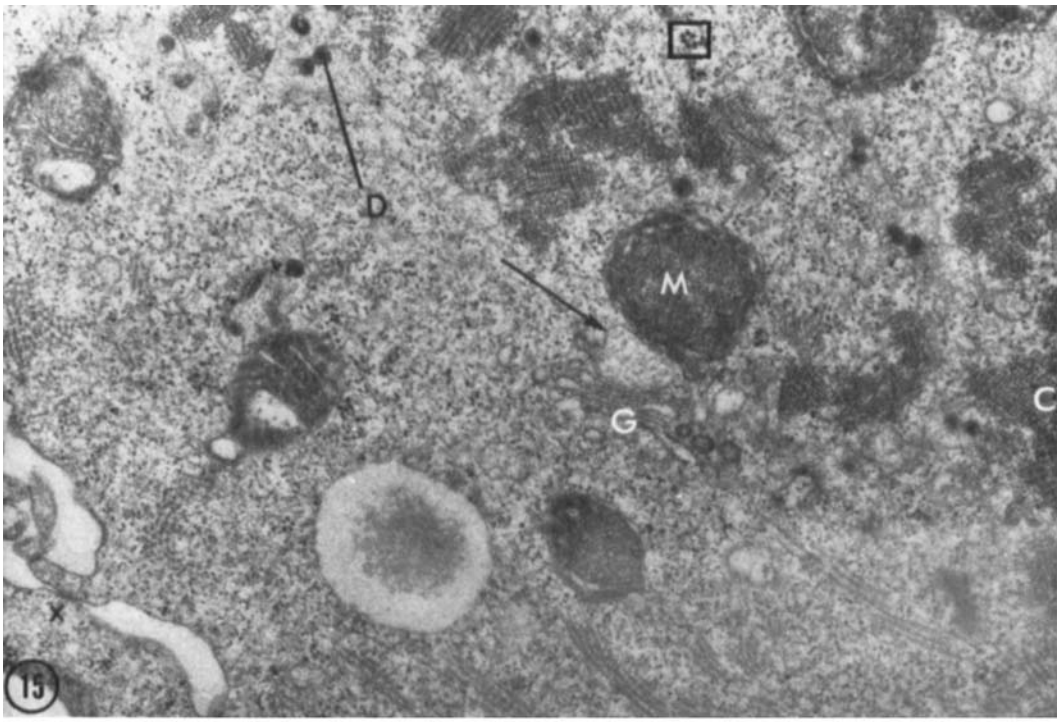
D
M
G
C
X
15

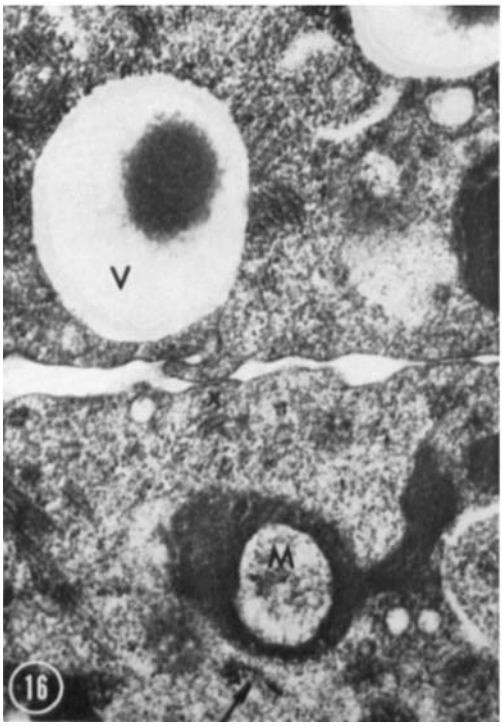
V
M
16

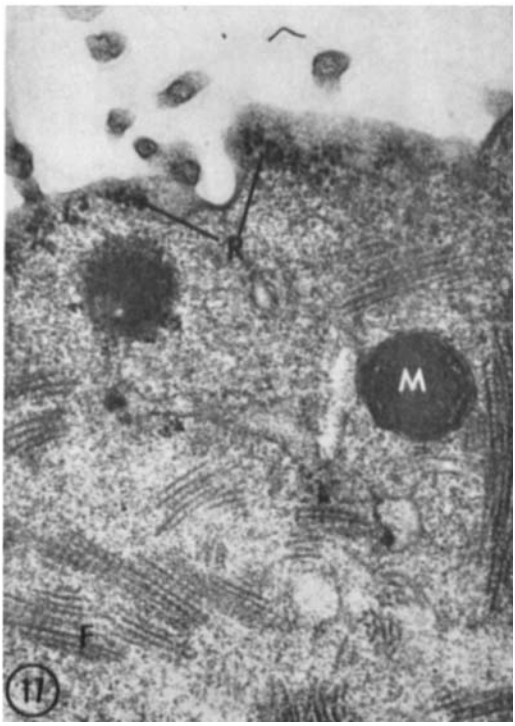
R
M
F
17

PLATE 5

EXPLANATION OF FIGURES

18 Two blastomeres of an eight-cell stage. Ribosomes are aligned along the cell margin (R) at the top of the micrograph, and the microvilli of the two cells are interdigitated. Large numbers of single "ribosomes" are present in the cytoplasm. V, cytoplasmic vesicle; M, mitochondrion. × 30,150.

19 Intercellular boundary between two blastomeres near the periphery of a morula. Note the localization of ribosomal clusters (R) along one side of this boundary. × 30,150.

20 Rough endoplasmic reticulum (ER) is seen in association with smooth membranous elements of the Golgi apparatus (G) in a blastomere at the morula stage. × 30,150.

21 Two blastomeres of a blastocyst. Note the difference in cytoplasmic background density between Cell A and Cell B. × 30,150.

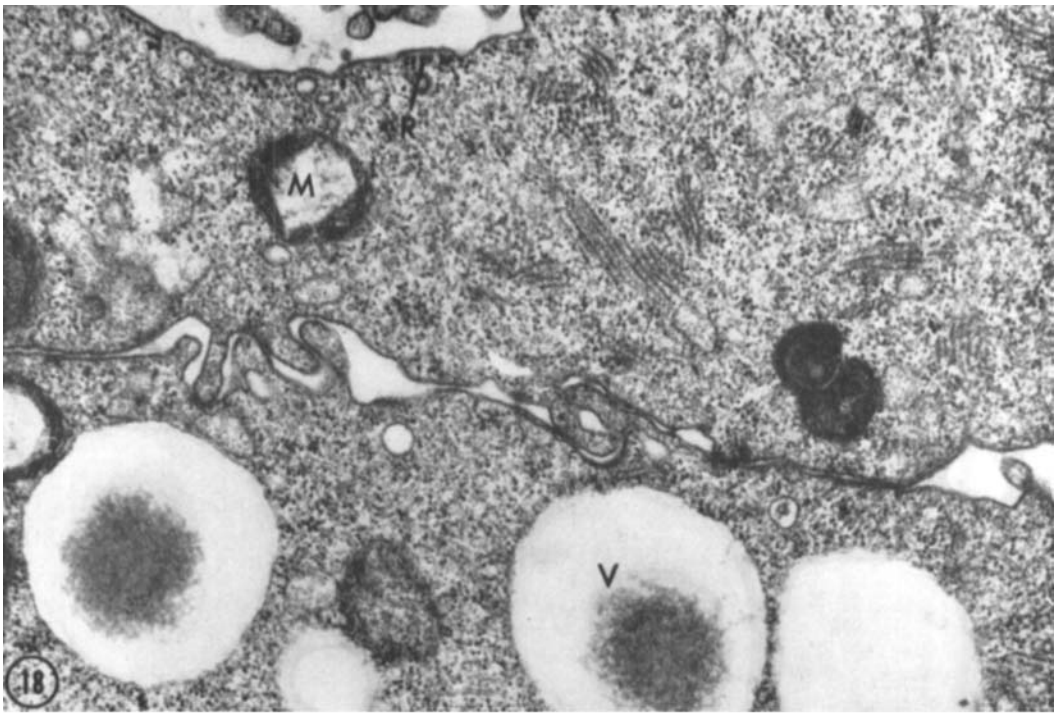
M
R
V
18

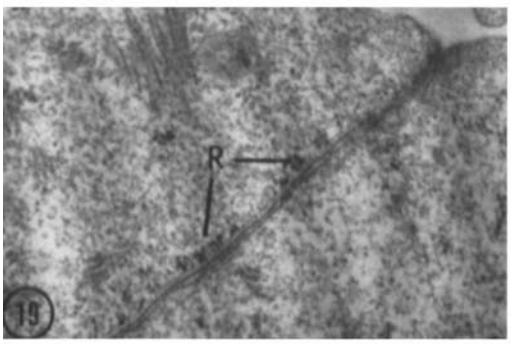
R
19

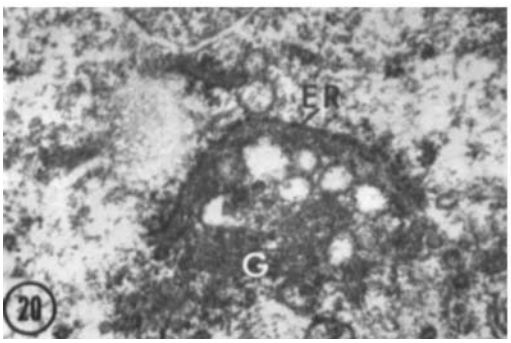
ER
G
20

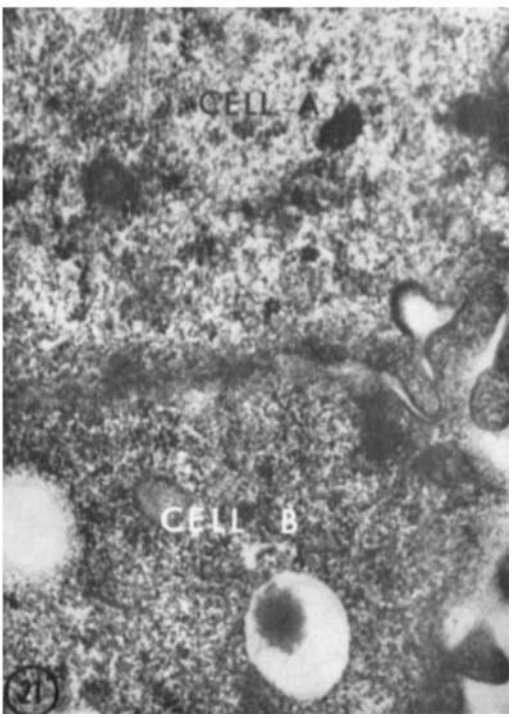
CELL A
CELL B
21

PLATE 6

EXPLANATION OF FIGURES

22 Unfertilized egg. Note the mitochondria in elongate and circular forms (M), the few cytoplasmic vesicles (V), which contain small amounts of medium-density material, and the large numbers of sacs (S). × 8,900.

23 Two mitochondria in an 8-cell stage. The arrow indicates a helical filament located within the intracristal space. C, crystalloid material. × 60,300.

24 A vesicle aggregate, perhaps derived from a multivesicular body, near the periphery of an unfertilized egg. M, mitochondrion. × 30,150.

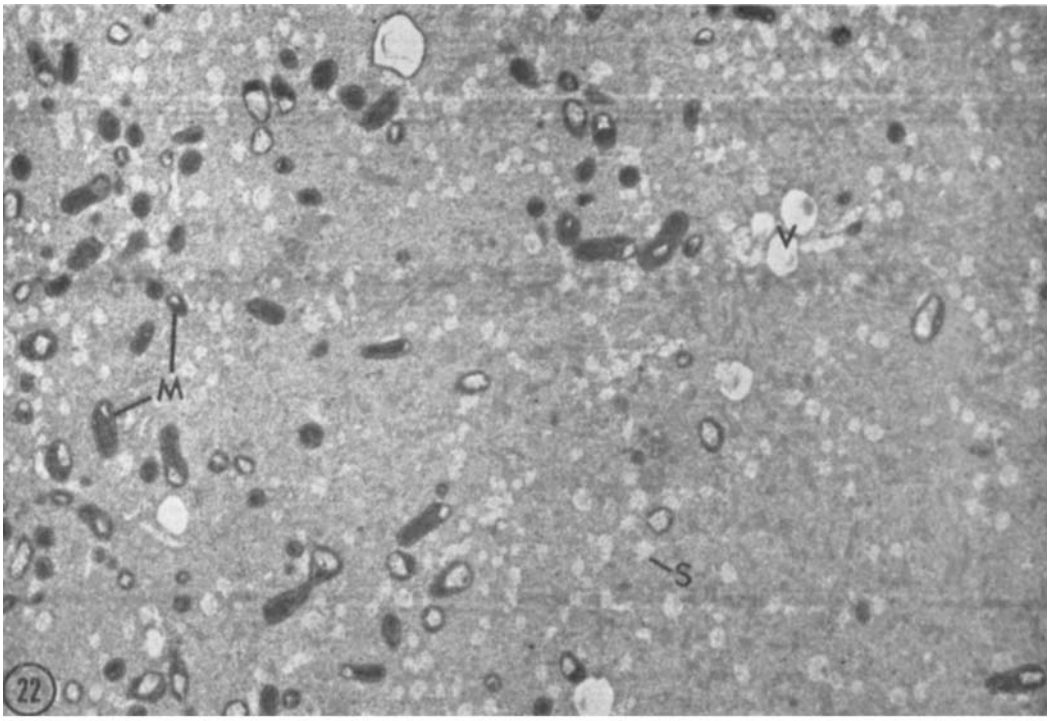
M
V
S
22


C
23

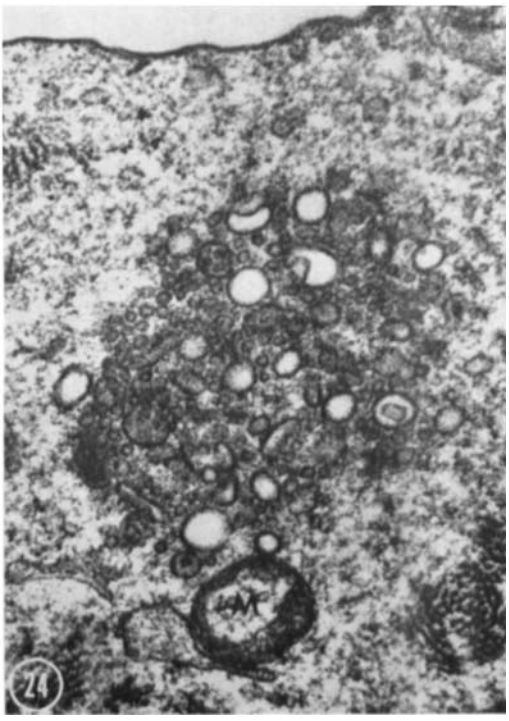
24

PLATE 7

EXPLANATION OF FIGURES

25 A cytoplasmic region at the 2-cell stage. J, aggregate of "jigsaw" vesicles; M, mitochondrion; V, cytoplasmic vesicle. × 30,150.

26 Tight junction, or junctional complex, (T) between two trophoblast cells of a blastocyst. The arrow indicates the lock-and-key interdigitations of these cells with a cell of the inner cell mass which is at the left of the figure. × 30,150.

27 The tight junctions (T) extend over a considerable length of attachment between the peripheral cells (presumptive trophoblast) and an internal cell in this morula. F, fibrous material. × 30,150.

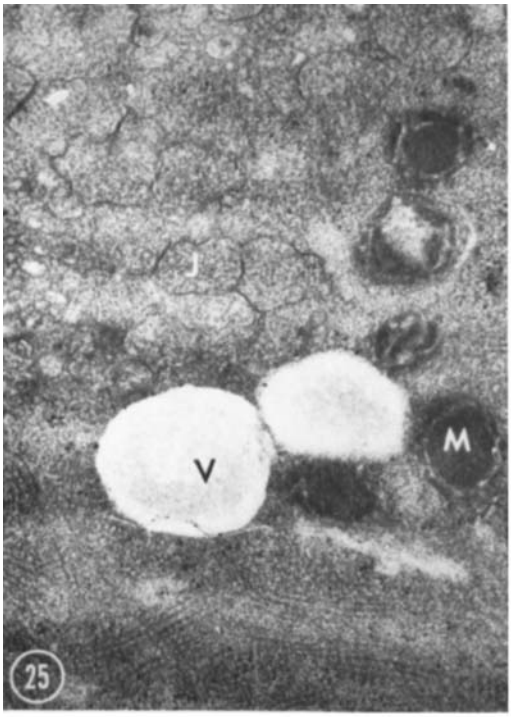
J
V
M
25

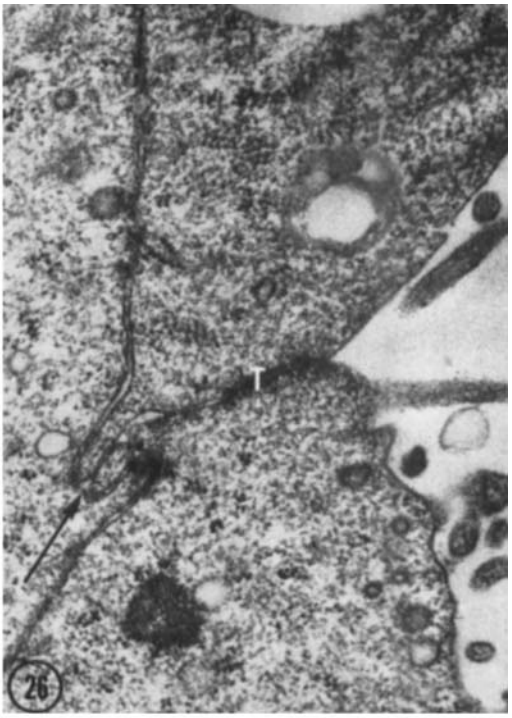
T
26

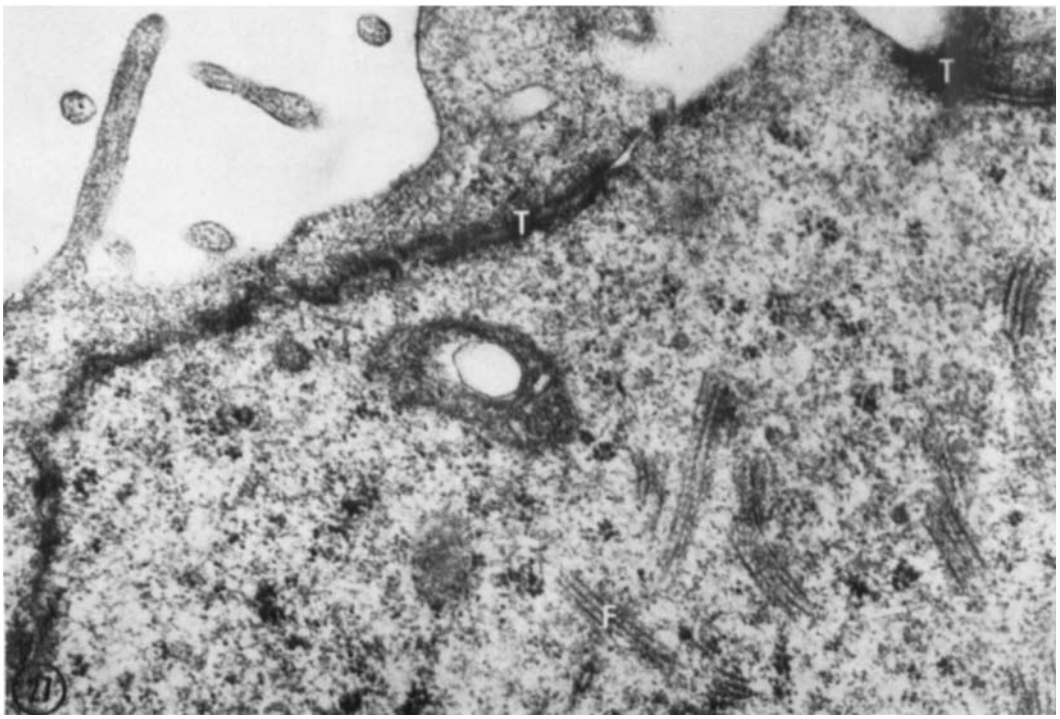
T
T
F
27

PLATE 8

EXPLANATION OF FIGURES

28 Part of a pronucleus of a fertilized egg. "N," spherical agranular "nucleoulus;" Ch, associated chromatin; IAL, intranuclear annulate lamellae; C, small area of crystalloid material in the cytoplasm. × 20,100.

29 Pronuclear extrusion sacs (P) at the boundary of a pronucleus of a fertilized egg. "N," "nucleolus;" M, mitochondrion; C, crystalloid. × 30,150.

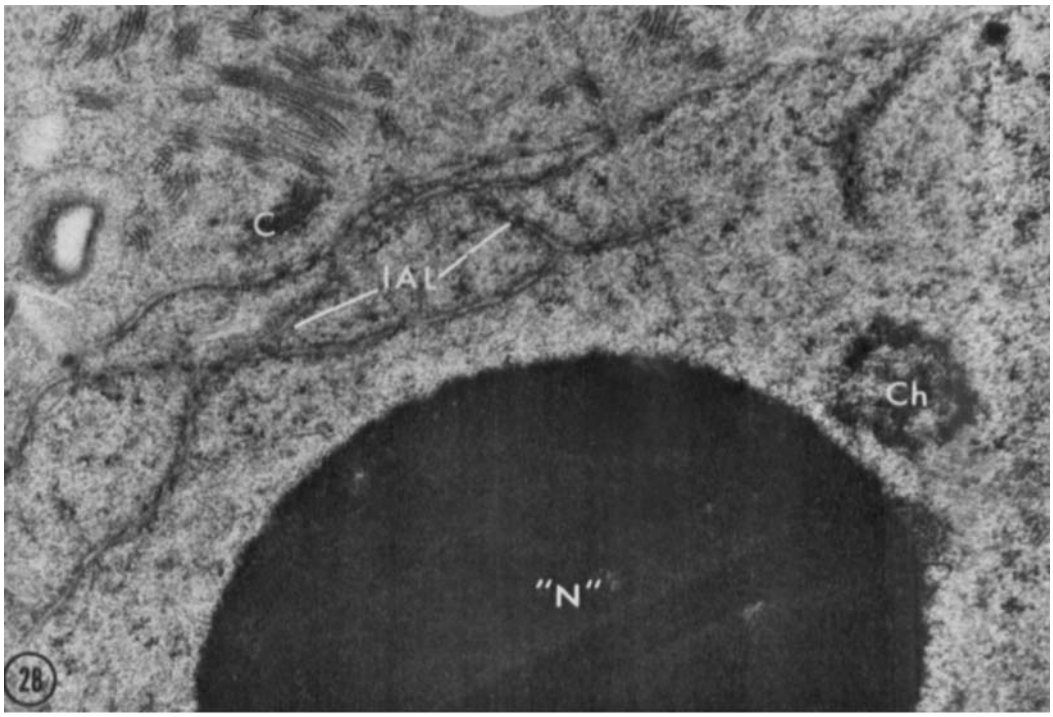
C
IAL
Ch
"N"
28

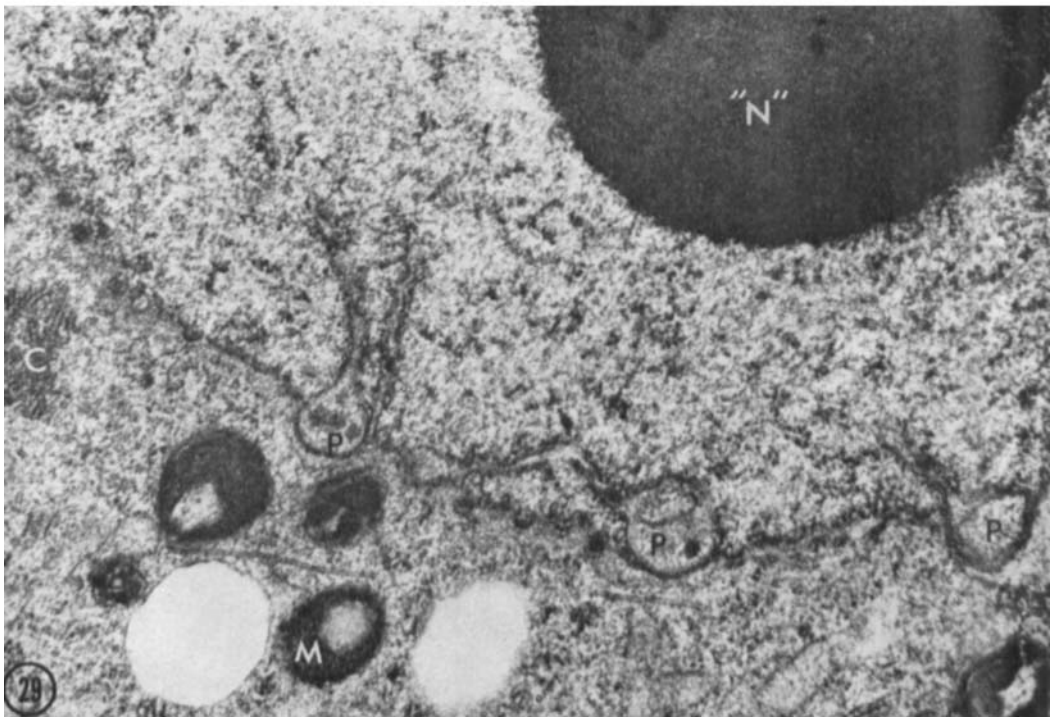
"N"
C
P
P
P
M
29

PLATE 9

EXPLANATION OF FIGURES

30 Nucleolus of an 8-cell stage. The nucleolonema (Nu), exhibiting granular and fibrillar regions, surrounds a spherical agranular body (N). Cy, cytoplasm. × 30,150.

31 Nucleolus in an early blastocyst nucleus. An intranuclear annulate amella (IAL) is evident. The small medium-density bodies may represent partes amorphae. × 20,100.

32 Two blastomeres of an 8-cell stage. Note that the lower margin of the cytoplasmic vesicle (V) is very close to, and may be continuous with, the intercellular space. M, mitochondrion; G, Golgi material. × 30,150.

33 A portion of an unfertilized egg showing large numbers of light-staining sacs (S) with ill-defined margins and containing light-staining strands. Some sacs are in association with mitochondria (M). V, cytoplasmic vesicles. × 20,100.

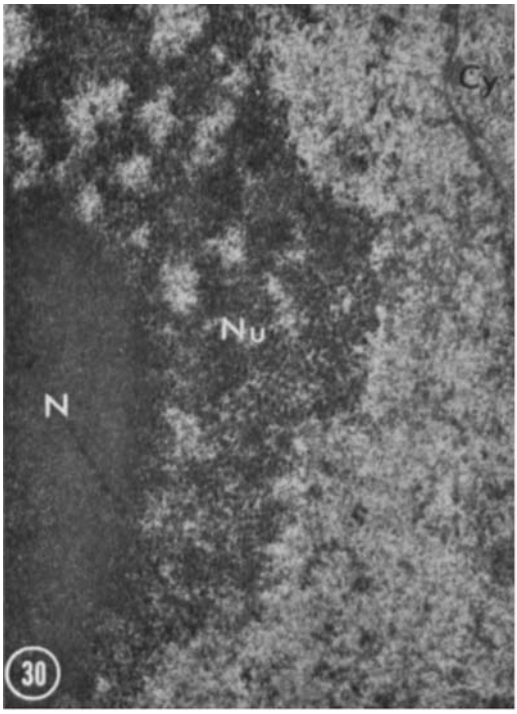
Cy
Nu
N
30

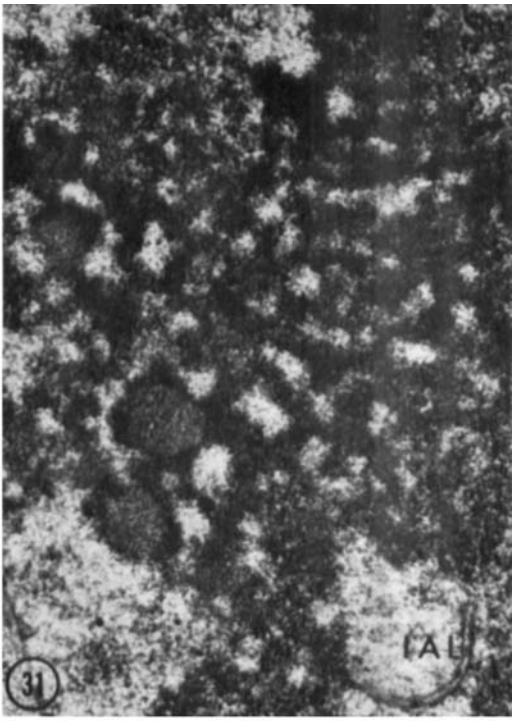
CAL
31


M
G
V
32

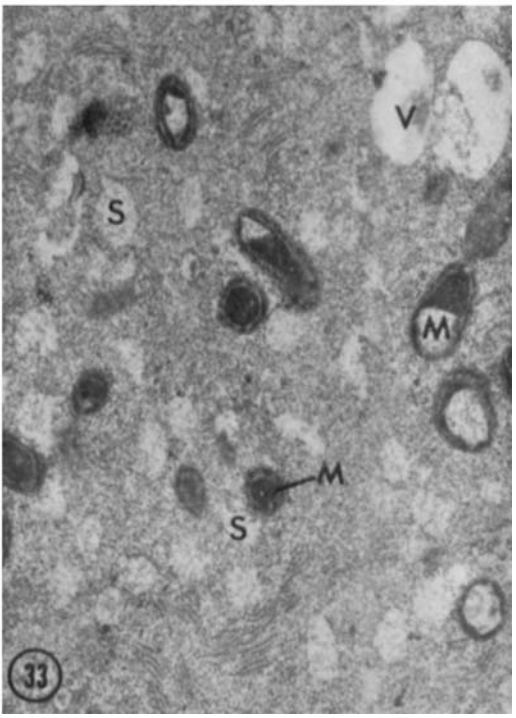
V
S
M
M
S
33